Effect of the range of attractive interactions on crystallization, metastable phase transition, and percolation in colloidal dispersions

Dong Fu and Yigui Li
Department of Chemical Engineering, Tsinghua University, Beijing 100084, People's Republic of China

Jianzhong Wu*
Department of Chemical and Environment Engineering, University of California, Riverside, California 92521, USA

(Received 26 February 2003; published 14 July 2003)

The equilibrium as well as nonequilibrium phase behaviors of colloidal dispersions have been investigated using statistical-mechanical theories of fluids and solids in complement with the renormalization-group (RG) theory. It is shown that the osmotic second virial coefficient at the critical point of the fluid-fluid transition varies with the range of attractions and is sensitive to specific forms of the attractive potential in contrast to a common speculation that it remains practically constant. However, for colloids with short-ranged forces, the critical temperature of the fluid-fluid phase transition is well correlated with the range of attractions in good agreement with an earlier empirical correlation based on simulation results. A comparison of the relative positions of the fluid-fluid coexistence curve, freezing, melting, and percolation lines in the phase diagram indicates that the gelation in colloidal systems has significant effects on the equilibrium phase transitions and crystallization, especially when the attractions between colloidal particles are short ranged.

DOI: 10.1103/PhysRevE.68.011403 PACS number(s): 82.70.Dd

I. INTRODUCTION

The phase behavior of colloidal dispersions has been of considerable interest in recent years for its close connection to that of atomic systems, to protein crystallization and for the broad applications of colloids in the fabrication of nanostructured materials including photonic crystals, advanced catalysts, membranes, and ceramics [1–10]. It is now well established that structural ordering in a colloidal dispersion resembles the fluid-solid transition in an atomic system, while the equilibrium between a dilute and a concentrated colloidal phases resembles the gas-liquid coexistence of a simple fluid. However, unlike that in most atomic systems where the intermolecular attractions are approximately conformal, attractions between colloidal particles vary widely depending on the chemical constitutes of the particles as well as on the solution conditions, such as temperature, pH, salt type, and solvent composition [11–15]. The lack of conformality in colloidal potentials complicates the phase behavior of colloids, especially on the interplay among various coexisting phases and nonequilibrium phase transitions [8,16–18].

Since the pioneering work by Gast, Hall, and Russel on the phase behavior of colloid-polymer mixtures [19], it has been extensively shown by theory [20–23], simulation [24–27], and experiment [28–30] that colloidal dispersions exhibit stable vapor-liquid-like transition when the attractive forces between colloidal particles are long ranged, and the fluid-fluid transition is metastable relative to the fluid-solid equilibrium when the attractions are short ranged. Approximately, the minimum range of attractions for the appearance of a thermodynamically stable fluid-fluid transition is about one-sixth of that of repulsions [31]. While previous investigations explain semiquantitatively why a condensed fluid (''liquid'') is thermodynamically stable in most atomic and molecular systems (where the van der Waals attractions between molecules are long ranged in comparison to the molecular diameter) and why the fluid-fluid transition in colloids is often metastable (owing to the large size of colloidal particles), there is only limited understanding of the relations between the stable or metastable thermodynamic phase transitions and a variety of loosely defined nonequilibrium colloidal phenomena such as gelation, coagulation, dynamic arrest, ergodic-nonergodic transitions, vitrification and jamming [32]. These nonequilibrium phenomena directly affect the behavior of equilibrium phase transitions in colloidal dispersions, structural ordering in particular, and often result in poorly characterized amorphous soft materials. Because of the interference of nonequilibrium phenomena, it is notoriously difficult to design experimental parameters to achieve desired equilibrium colloidal structures such as crystallization of aqueous protein solutions that are of significant importance in practical applications.

Nonequilibrium states such as gels, aggregates, and glasses are commonplace in colloidal systems and they play important roles in materials, food, medical, and numerous other industries [33]. However, the lack of a coherent understanding of these nonequilibrium states means that many industrially important processes are handled by strictly empirical means. Although much progress has been made in recent years on the dynamic behavior of colloidal dispersions, it remains difficult to provide accurate predictions of various nonequilibrium phenomena [32,34,35]. The most successful theoretical approach to describe glass transition in colloidal systems is from the ideal mode coupling theory (MCT) [36,37]. MCT provides a good representation of the dynamic structure factors of hard-sphere and charge-stabilized colloids as well as in colloids with short-ranged attractions near glass transition [17,38–41]. While MCT explains some elements of the transition to nonequilibrium states, it does suffer

*Author to whom correspondence should be addressed. Email address: jwu@engr.ucr.edu

severe limitations, especially at conditions where the system is thermodynamically unstable and the definition of the equilibrium structure factor lacks a clear physical meaning. Recently, MCT has also been proposed to represent the glassy behavior of colloidal gelation [8].

In this work, we investigate the interplay of the equilibrium phase transitions and the percolation in colloidal systems with changeable ranges of interparticle attractions. We consider here two model potentials commonly used in the literature. One is the hard-core attractive Yukawa potential where the interparticle attraction decays exponentially with the separation. The other is the Asakura-Oosawa potential, which is frequently used to represent the interaction between colloidal particles in the presence of nonadsorbing polymers. We choose these two model systems because their equilibrium phase diagrams are relatively well understood and there has been fair amount of evidence on the behavior of their nonequilibrium states. Nevertheless, even for these relatively simple systems, a quantitative representation of the complete phase diagram, especially on the interactions among fluid-fluid, fluid-solid phase transitions and gelation, remains subtle. Over the past few years there have been speculations based on experimental observations [42] and molecular simulations for various model potentials [43] that the metastable fluid-fluid coexistence curve is likely to be represented by an extended corresponding state theory. It has also been conjectured that the reduced osmotic second virial coefficients at the critical point of the metastable fluid-fluid equilibrium remain practically constant for a variety of colloidal dispersions [44]. Furthermore, empirical correlations have been proposed that relate the second virial coefficient to the critical temperature of the metastable fluid-fluid transition [43] and to the solubility and crystallization of proteins in aqueous solutions [9,45]. However, little theoretical investigations have been reported to verify these and other postulates that are obtained from limited experimental and simulation data.

Prediction of the fluid and solid boundaries requires reliable thermodynamic models for both crystalline solids and fluid phases. While the liquid-state theories are now well established, it remains challenging to predict the thermodynamic and structural properties of crystalline phases and fluid properties near the critical region. Our calculations in this work are based on recently developed perturbation theories for the fluid and solid phases and on a percolation theory for potential colloidal gelation. We use different thermodynamic models for the fluid and solid because there is no continuous phase transition between the two phases. As long as both theoretical models are adequate, we should have accurate fluid-solid coexistence curves. Near the critical point of the fluid-fluid transition, we use a renormalization group theory originally proposed by White and co-workers [46,47] to take into account the long-range fluctuations. The calculated equilibrium phase diagrams are compared with simulation data whenever they are available. Meanwhile, a relatively simple theory of colloidal percolation proposed recently by Noro and Frenkel [16] is applied to predict the potential gelation regions. This theory is based on an earlier work for the percolation of adhesive hard spheres developed by Chiew and Glandt [48]. While the numerical accuracy of this theory is yet to be established, it provides at least useful insights into the relation between the gelation and the metastable fluid-fluid transition that qualitatively agree with experimental observations.

II. THEORY

In this section, we briefly discuss the theoretical models used in the investigation of the equilibrium phase diagrams and the percolation of Yukawa as well as Asakura-Oosawa model systems.

A. Yukawa fluids

The hard-core attractive Yukawa potential is given by

$$u^Y(r)=\begin{cases}\infty, & r<\sigma\\ -\varepsilon\dfrac{\exp[-\kappa(r-\sigma)]}{r/\sigma}, & r\geqslant\sigma,\end{cases}\tag{1}$$

where r is the center-to-center distance between particles and σ is the hard-core diameter. The energy parameter ε in the Yukawa potential specifies the strength of attraction and the screening parameter κ defines the attraction range. According to Eq. (1), the attraction becomes longer ranged as the screening parameter κ of the Yukawa potential decreases.

A variety of statistical-mechanical theories are available to represent the thermodynamic properties of Yukawa fluids [49]. The most common approach is from the mean-spherical approximation (MSA), which provides analytical expressions for both structural and thermodynamic properties [50]. The reference hypernetted chain (HNC) approximation [51] and the self-consistent Ornstein-Zernike approximation (SCOZA) [17] are more accurate than MSA but require significantly more numerical efforts. In this work, we use a variation of the MSA proposed recently by Henderson and co-workers based on the inverse temperature expansion of the Helmholtz energy up to the fifth order [52,53]. We used the modified MSA instead of the first-order perturbation theory because the later is not very accurate when the attraction is long ranged. Unlike the original MSA where a set of six equations must be solved numerically, the modified MSA gives completely analytical expressions for the equation of state as well as for the radial distribution functions. Except near the critical point of the vapor-liquid equilibrium, the calculated results agree favorably with simulation data.

The Helmholtz energy according to the modified MSA can be expressed as [54]

$$\frac{A}{NkT}=\frac{4\eta-3\eta^2}{(1-\eta)^2}-\frac{\theta_0}{\Phi_0}\frac{\varepsilon}{kT}-\frac{(\kappa\sigma)^3}{6\eta}\times\left[F(x)-F(y)-(x-y)\frac{dF(y)}{dy}\right],\tag{2}$$

where k is the Boltzmann constant, T is the temperature, and N is the number of particles. The first term on the right-hand side of Eq. (2) is the reduced Helmholtz energy for the hard-

sphere reference fluid given by the Carnahan-Starling equation of state [55]. The packing faction is defined as $\eta = (\pi/6)\rho\sigma^3$, where ρ stands for the particle number density. The remaining terms on the right-hand side of Eq. (2) are the reduced Helmholtz energy from the modified MSA for the attractive potential. Appendix A gives the expressions for the parameters θ_0, Φ_0, the single-variable function $F(x)$, and the variables x and y. Equation (2) provides the starting point for calculating the vapor-liquid equilibrium of the Yakawa fluid using the renormalization group (RG) theory (see Sec. III D). Recently the modified MSA has been used to describe the thermodynamic properties of a variety of nonpolar fluids [56] and phase behavior of aqueous colloidal dispersions [57].

B. Asakura-Oosawa fluids

Asakura-Oosawa (AO) model is conventionally used to present the equilibrium phase behavior of colloids containing nonadsorbing polymers [23,26,58]. According to this model, colloidal particles are represented by hard spheres and polymers by ideal chains that do not interact with each other. While the ideal polymer chains are allowed to penetrate among themselves, they are excluded from the particle surface, i.e., the center of mass of a polymer chain is separated from the particle surface no closer than the polymer radius of gyration. Due to the entropy effect, the excluded volume of the ideal polymers results in an effective attraction between colloidal particles, which can be represented by the Asakura-Oosawa potential [59]

$$u^{\mathrm{AO}}(r) = \begin{cases} -\eta_p kT\left(\dfrac{1+\delta}{\delta}\right)^3 [1 - a_1(r/\sigma) + a_2(r/\sigma)^3], & \sigma \leqslant r < +\sigma_p \\ 0, & r \geqslant \sigma + \sigma_p, \end{cases} \tag{3}$$

where σ is the hard-sphere diameter of the colloidal particle, σ_p is twice of the radius of gyration of the polymer chain, $\delta = \sigma_p/\sigma$ is the polymer-particle size ratio, and $\eta_p = \pi\sigma_p\rho_p/6$ is the packing fraction of the polymer at a number density ρ_p. In Eq. (3), the coefficients a_1 and a_2 are given by $a_1 = 1.5/(1+\delta)$ and $a_2 = 0.5/(1+\delta)^3$. The Asakura-Oosawa potential was originally derived from geometric considerations and can also be derived from statistical mechanics [60]. According to this potential, the strength of attraction between colloidal particles is controlled by the polymer packing fraction and the range of attraction by the polymer radius of gyration.

Various statistical-mechanical theories for representing the thermodynamic properties of AO fluids have been recently reviewed by Poon [58]. Most of these theories vary in the way the polymer component is treated. In this work we follow the ''one-component'' approach where the pairwise additive potential is given by Eq. (3). The mean-field Helmholtz free energy of the fluid phase is represented by a first-order perturbation theory [19,49]:

$$\frac{A}{NkT} = \frac{4\eta - 3\eta^2}{(1-\eta)^2} + \frac{2\pi\rho}{kT}\int_\sigma^\infty u^{\mathrm{AO}}(r) g_0(r) r^2 dr, \tag{4}$$

where the radial distribution function of the hard-sphere reference system, $g_0(r)$, is given by an analytical solution of the Percus-Yevick (PY) equation proposed by Chang and Sandler [61]. We use the radial distribution function of hard spheres from Chang and Sandler instead of the widely used Verlet-Weis form [62] because the later requires numerical solution of the PY equation. We use the former because it is analytical. With the RG theory for correcting long-range fluctuations near the critical point of the fluid-fluid transition, we found that the second-order perturbation terms have only negligible effect on the calculated results for the vapor-liquid equilibrium of the AO fluids [63].

C. Crystalline solids

A recently proposed first-order perturbation theory is used to describe the thermodynamic properties of the Yukawa and AO solids [64]. As for the fluid phase, the Helmholtz energy includes a contribution from the reference hard-sphere crystal and a perturbation term taking into account the attractive interactions

$$\frac{A}{NkT} = \frac{A^{HS}}{NkT} + 12\eta\sigma^{-3}\int_\sigma^\infty r^2 g_S^{HS}(r)\frac{u_A(r)}{kT}dr, \tag{5}$$

where $g_S^{HS}(r)$ is the radial distribution function of the hard-sphere solid, and $u_A(r)$ is the attractive potential given by Eq. (1) or (3). We assume that as in the hard-sphere reference system, the solid phases of both Yukawa and AO model systems have a face-centered-cubic (FCC) structure. The body-center-cubic (BCC) structure is stable only when there is long-range attraction between particles.

The Helmholtz energy of the hard-sphere solid is given by a modified cell mode [65],

$$\frac{A^{HS}}{NkT} = -\ln\left\{\frac{8}{\sqrt{2}}[(\rho/\rho_0)^{1/3} - 1]\right\}, \tag{6}$$

where $\rho_0 = \sqrt{2}/\sigma^3$ is the close packing density of a FCC crystal. Compared with the original cell model proposed many years ago by Lennard-Jones and Devonshire [66], the modified cell model introduces a factor of 8 on the left-hand side of Eq. (6), taking into consideration that in real crystals the neighboring particles partially share the free space between

lattice sites. Unlike the original cell model, the modified cell model provides accurate freezing and melting densities for the fluid-solid transition of uniform hard spheres.

To obtain the radial distribution function of hard spheres in an FCC lattice, we use a procedure similar to that proposed by Rascon, Mederos, and Navascues [67]. The radial distribution function around an arbitrary tagged particle can be represented by the summation of an empirical exponential function for the first layer and the Gaussian distributions in the remaining layers:

$$g_S^{HS}(r') = \frac{\alpha_0}{r'} e^{-\alpha_1 (r'-R_1)/2} + \frac{1}{24\eta}\sqrt{\alpha/2\pi} \times \sum_{i\geq 2} \frac{n_i}{r' R_i} [e^{-\alpha (r'-R_i)/2} + e^{-\alpha (r'+R_i)/2}], \quad (7)$$

where $r' = r/\sigma$, n_i is the number of particles in the ith neighboring layer from the tagged particle, R_i represents the center-to-center distance between a particle in the ith layer and the tagged particle. For an FCC lattice, the Gaussian parameter α is related to the overall particle number density by [68]

$$\alpha = \left(\frac{\sqrt{3}\pi}{4}\right)^{2/3} \left[\left(\frac{\sqrt{2}}{\rho\sigma^3}\right)^{1/3} - 1\right]^{-2}. \quad (8)$$

Equation (8) is derived from a comparison between the free volumes from the cell model and from the Gaussian density distributions [68]. Other parameters in Eq. (7), α_0, α_1, and R_1 are determined by requiring that the radial distribution function gives the exact number of particles within the first layer, the exact mean distance between immediate neighboring particles, and a contact value that is consistent with the corresponding equation of state. By imposing these requirements, the parameters α_0, α_1, and R_1 can be solved from

$$4\pi\rho\alpha_0 \int_1^\infty r' e^{-\alpha_1 (r'-R_1)/2} dr' = n_1, \quad (9)$$

$$\frac{4\pi\rho}{n_1} \int_1^\infty r'^2 e^{-\alpha_1 (r'-R_i)/2} dr' = R_1, \quad (10)$$

$$Z = 1 + 4\eta\alpha_0 e^{-\alpha_1 (1-R_1)/2}, \quad (11)$$

where Z stands for the compressibility factor of the hard-sphere solid, which, according to the modified cell model, is given by

$$Z = 1/[1 - (\rho\sigma^3/\sqrt{2})^{1/3}]. \quad (12)$$

In this work, we assume that the correlation beyond the first five layers does not make significant contribution to the thermodynamic properties. The numbers of particles (n_i) in the first five layers around an arbitrarily selected particle at the FCC lattice are given by [69]

$$(12,6,24,12,24) \quad (13)$$

and the corresponding distances (R_i) from the central particle in units of lattice constant are

$$(1,\sqrt{2},\sqrt{3},\sqrt{4},\sqrt{5}). \quad (14)$$

We use R_1 from Eq. (10) and R_i, $i=2,3,4,5$, from Eq. (14) to calculate $g_S^{HS}(r)$, as given in Eq. (7). Once we have the radial distribution function for the hard-sphere solid, the perturbation term in Eq. (5) can be integrated numerically using the Romberg adaptive method.

D. Renormalization group theory

Although recent advances in equilibrium theory of simple fluids have been primarily focused on the critical behavior near the vapor-liquid transition [70], we are not aware of any published work applying similar theories for colloidal systems. However, experimental investigations on the phase behavior of colloidal dispersions and aqueous protein solutions are often in the vicinity of the critical point of the metastable fluid-fluid phase transition [42,71,72]. Indeed, nonmean-field scaling law on the relation between the critical temperature and the density has been observed in aqueous protein solutions. As first discovered by tenWolde and Frenkel using Monte Carlo simulations [73] the fluid-fluid critical point is directly related to the dynamics of colloidal-protein crystallization and dictates whether the fluid-fluid phase transition is metastable or stable in comparison to the fluid-solid equilibrium.

It is well recognized that a mean-field theory is not accurate for predicting the critical point of the fluid-fluid transition. Although the attraction between colloidal particles is typically shorter ranged than that between atomic molecules, the same theoretical tools for the nonmean-field behavior of simple fluids can be equally applied to colloidal systems in the framework of the ''one-component'' model. In this work, we use a RG theory originally developed by White and Zhang [47], taking into consideration the long-range fluctuations. Similar applications have been recently published for the vapor-liquid equilibrium of square-well and Lennard-Jones models as well as realistic fluids [74–76].

The RG theory calculates the Helmholtz energy due to long-range correlations recursively. It starts with a mean-field Helmholtz energy that ignores the fluctuations with a wavelength longer than λ_0. In this work, this mean-field Helmholtz energy is calculated from Eq. (2) or Eq. (4) for Yukawa fluids and for AO fluids, respectively. The initial mean-field Helmholtz energy corresponds to that in a phase-space cell of volume $V_{D,0} = \lambda_0^3$. Contributions to the Helmholtz energy density due to longer wavelength fluctuations are calculated by adding a sequence of corrections to the Helmholtz energy density, δf_n, $n=1,2,\ldots$. Specifically, as the fluctuation wavelength is increased at each step by a constant factor of t, the phase-space cell volume V_D is increased by a factor of t^3:

$$V_{D,n} = t^3 V_{D,n-1}, n = 1,2,..., \quad (15)$$

where $t=2$ is used in our calculations. The Helmholtz energy density after the expansion of the phase-space cell is calculated from a recursive relation

$$F_n(\rho)=f_{n-1}(\rho)+\delta f_n(\rho), \tag{16}$$

where the differential Helmholtz energy density $\delta f_n(\rho)$ is given in Appendix B. Two parameters L and ψ are involved in the RG recursion: L is related to the initial cutoff wavelength λ_0 and ψ stands for the average gradient of the wavelet function (see Ref. [74] for details). These two parameters are obtained by fitting to the simulation results. The final Helmholtz energy of the system is calculated from the Helmholtz energy density according to

$$A/V=\lim_{n\to\infty} f_n(\rho). \tag{17}$$

For most cases, satisfactory thermodynamic properties can be achieved after only a few steps of recursions.

E. Percolation theory for potential gelation

We use a simple percolation theory proposed by Noro and Frenkel [16] to identify the boundary of possible gelation in Yukawa and in AO systems. We select this theory to represent gelation because it involves only static properties of colloids and because it does not require the equilibrium structure factor as an input. The key assumption in this method is that the long-range attractions between colloidal particles have little effect on the threshold of percolation, and the boundary of possible gelation is mainly determined by an effective sticky parameter that represents the short-ranged attractions. The percolation criterion of Chiew and Glandt for sticky spheres is utilized to delimit the region where gelation is possible [48]. Percolation is a necessary but not a sufficient condition to form a gel.

The long- and short-range attractive potentials are separated in terms of the osmotic second virial coefficient

$$B_2=B_2^{HS}\left(1-\frac{1}{4\tau^{ss}}-\frac{1}{4\tau^{vdw}}\right), \tag{18}$$

where $B_2^{HS}=2\pi\sigma^3/3$ is the second virial coefficient of hard spheres, τ^{ss} is the sticky parameter defining the short-ranged attraction, and τ^{vdw} is an effective sticky parameter characterizing the long-ranged forces. The sticky parameter τ^{vdw} is related to the van der Waals energy parameter a by

$$\tau^{vdw}=kTv_0/a, \tag{19}$$

where $v_0=\pi\sigma^3/6$ is the hard-sphere volume. Noro and Frenkel conjectured that percolation in a colloidal system depends only on the short-range sticky parameter τ^{ss}, which according to the analysis of Chiew and Glandt for sticky hard spheres occurs when

$$\tau^{\infty}\leqslant\frac{1-2\eta+19\eta^2}{12(1-\eta)^2}. \tag{20}$$

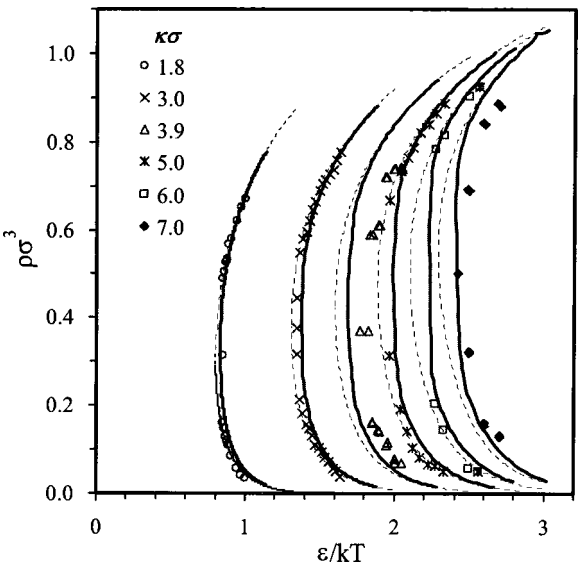

FIG. 1. Fluid-fluid coexistence curves for Yukawa fluids at various ranges of attractions. The solid and dashed lines are, respectively, calculated from the modified MSA theory with and without the RG corrections. The symbols are from Monte Carlo simulation by Hagen and Frenkel ($\kappa\sigma=3.9, 7.0$) [25] and by Shukla ($\kappa\sigma=1.8, 3.0, 5.0, 6.0$) [81].

By comparing the percolation line to the fluid-fluid coexistence curve calculated from a mean-field theory, Noro and Frenkel concluded that long-range attraction is essential to quench metastable fluid-fluid equilibrium in colloidal systems.

III. RESULTS AND DISCUSSIONS

The fluid-fluid and fluid-solid coexistence curves are calculated by imposing that the osmotic pressures and the chemical potentials of two coexisting phases be equal:

$$p^I=p^{II},$$

$$\mu^I=\mu^{II}. \tag{21}$$

For fluid-solid equilibrium, the osmotic pressures and the chemical potentials are directly calculated from the corresponding Helmholtz energies for fluid and solid phases using the standard thermodynamic identities

$$p/\rho kT=\rho\left[\frac{\partial(A/NkT)}{\partial\rho}\right]_{N,T}, \tag{22}$$

$$\mu/kT=\left[\frac{\partial(\rho A/NkT)}{\partial\rho}\right]_{V,T}. \tag{23}$$

For fluid-fluid equilibrium, the RG theory is used to calculate the Helmholtz energy. The boundary for possible gelation is located by using Eq. (20).

A. Fluid-fluid and fluid-solid coexistence curves

Figure 1 presents the calculated fluid-fluid coexistence

curves of attractive hard-core Yukawa model, using the modified MSA and the RG theory. Here the range of attraction varies from $\kappa\sigma=1.8$ (long-ranged) to 7 (short-ranged). The critical point for each $\kappa\sigma$ is solved from the first and second derivatives of the osmotic pressure with respect to density. As in the previous applications of RG theory for simple fluids [74,75,77], we treat ψ and L as adjustable parameters. In Fig. 1, ψ and L are set to be 10.0 and 0.6σ, respectively. We found that these values yield the best fit of the critical temperatures and coexisting curves from Monte Carlo simulations. Figure 1 shows that the agreement between calculated results and simulation data is satisfactory at both short and long ranged attractions. While the coexistence curves calculated from the modified MSA theory alone agree well with simulation results far from the critical region, the modified MSA significantly overpredicts the critical temperatures. Figure 1 indicates that while the critical density is relatively insensitive to the change of the range of attraction, there is an apparent increase in the critical temperature as the range of attractions rises.

Figure 2 shows the interaction between the fluid-fluid transition and the fluid-solid transition of the Yukawa model system for three values of $\kappa\sigma$. When the attraction is long ranged [Fig. 2(a), $\kappa\sigma=3.9$], the fluid-fluid phase transition is thermodynamically stable in comparison to the fluid-solid transition. In this case, the phase diagram includes a triple point where a dilute solution (vapor), a concentrated solution (liquid), and a crystalline solid are at equilibrium. As expected, the RG correction has only a minor effect at the triple point as long as it is not near the fluid-fluid critical region. As the range of attraction is reduced [Figs. 2(b) and 2(c), $\kappa\sigma=7$ and 9, respectively], the fluid-fluid coexistence curve lies underneath the freezing line, denoting that the fluid-fluid transition is metastable. Both Figs. 2(b) and 2(c) indicate that the calculated freezing and melting lines are in good agreement with simulation results, particularly in the limit of high temperature. When $\varepsilon/kT=0$, the system reduces to a hard-sphere colloid. Most previous investigations on fluid-solid equilibrium are based on perturbation theories similar to those present in this work. However, because the original cell model for hard-sphere phase transition is not at all accurate, simulation results for the freezing and melting densities are used as a reference for systems with attractive forces. Unlike most previous investigations of fluid-solid equilibrium, our calculations do not require the simulation results for the freezing transition of hard spheres.

Similar calculations have been applied to the AO fluids. Figure 3 shows the fluid-fluid and fluid-solid coexistence curves for three values of the colloid-polymer relative diameters. Also included in Fig. 3 are molecular simulation results by Tavares and Sandler, using the pairwise additive AO potential [63]. We did not include in this plot the fluid-fluid coexistence lines at small values of polymer-particle size ratios because the simulation data are not available. With the RG parameters ψ and L set as $\psi=7.5$ and $L/\sigma=1.0$, the calculated fluid-fluid coexistence curve is in excellent agreement with simulation results for $\delta=1$. In this case, the agreement between calculated and simulated melting and freezing lines is also satisfactory. At smaller values of δ, however, the

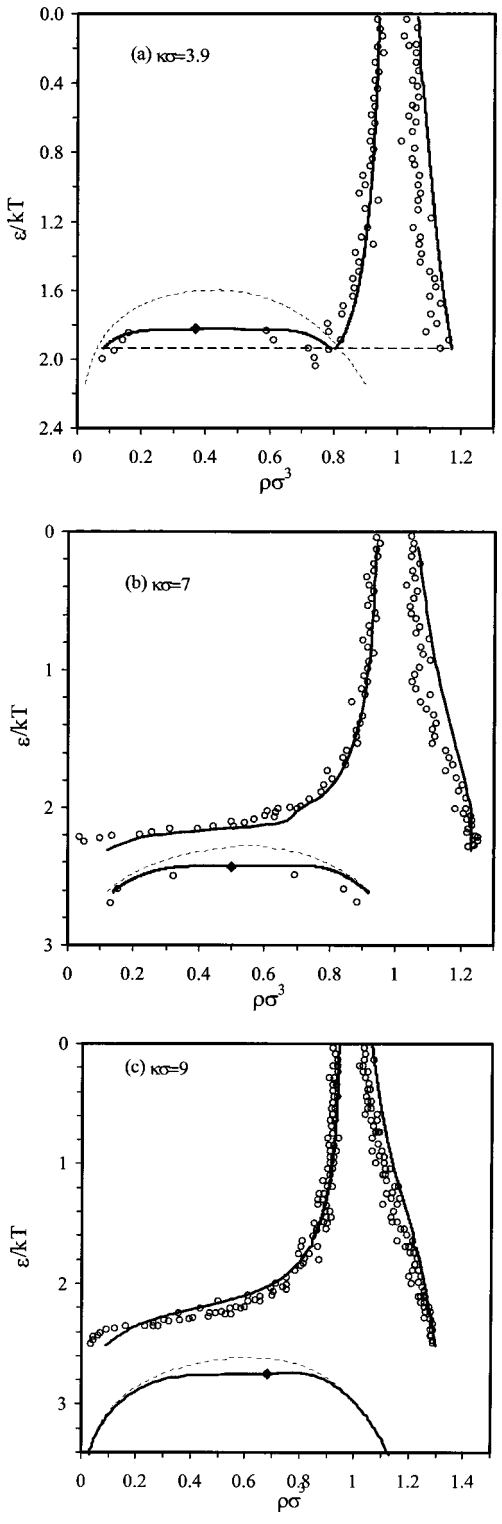

FIG. 2. Phase diagrams for the Yukawa system at three different ranges of the attractive interactions. (a) $\kappa\sigma=3.9$, the fluid-fluid coexistence is thermodynamically stable; (b) $\kappa\sigma=7.0$; and (c) $\kappa\sigma=9.0$, the fluid-fluid phase transitions are metastable. The solid lines and cycles are fluid-fluid and fluid-solid coexistence curves calculated from the theory and simulation, respectively. The dashed lines are fluid-fluid coexistence curves according to the modified MSA theory without RG correction. The diamonds correspond to the critical points calculated from Monte Carlo simulation [25].

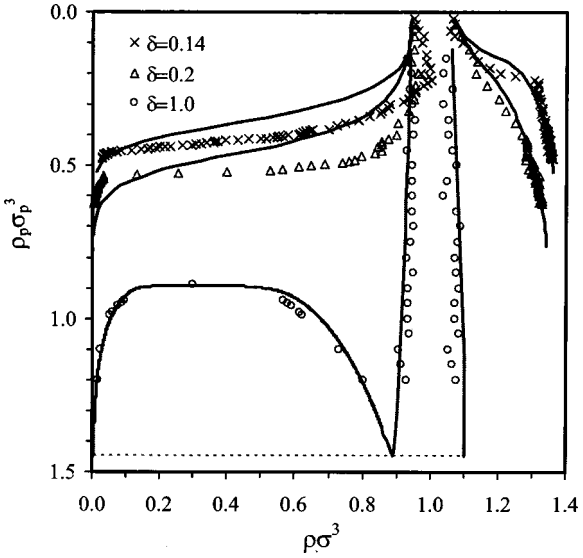

FIG. 3. Phase diagrams for the Asakura-Oosawa system of different ranges of attractions. The solid lines and symbols are fluid-fluid and fluid-solid coexistence curves calculated from the theory and simulation, respectively. Here the simulation data are from Tavares and Sandler [63].

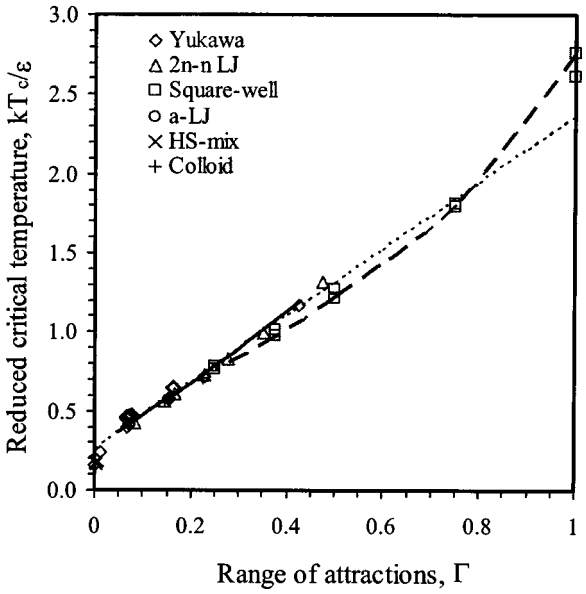

FIG. 4. The effect of the range of attractions on the reduced critical temperature of the fluid-fluid equilibrium for various model potentials. The simulation results are from Noro and Frenkel [43] and from Vliegenthart and Lekkerkerker [44], the solid and dashed lines are calculated results using the RG theory for the Yukawa potential and for the square-well potential, the dotted line is an empirical correlation proposed by Noro and Frenkel [43]. The RG results for the square-well potential are from Lue and Prausnitz [74].

perturbation theory gives only a fair account of the freezing lines. Similar observations have been reported in previous investigations on the phase behavior of AO fluids [26,63]. As for the Yukawa system, the AO potential yields a stable fluid-fluid phase transition when the attraction is long ranged (large size of polymer chains) and a metastable fluid-fluid transition when the attraction is short ranged (small size of polymer chains).

B. The critical point of the fluid-fluid transition

A few year ago Rosenbaum and co-workers reported that when the phase diagrams of some aqueous protein solutions and colloidal dispersions are plotted in terms of the sticky parameter (or effectively, the reduced second virial coefficient) and the reduced number density, the fluid and solid lines of different colloids fall remarkably close as in the corresponding state theory of simple fluids [42]. More recently, Vliegenthart and Lekkerkerker showed that although the critical temperature is sensitive to the range of attractive interactions, the reduced osmotic second virial coefficient remains practically constant at the critical point [44]. Based on these and other investigations on the critical behavior of colloidal dispersions, it has been speculated that the fluid-fluid coexistence curves of colloidal dispersions may follow an extended corresponding theory [43]. Semiempirical correlations have also been proposed as a predictor for protein crystallization and for the solubility of proteins in aqueous solutions [9,45]. While these and other semiempirical correlations appear in good agreement with a variety of simulation results and experimental data, little theoretical investigations have been reported on the critical temperatures of colloidal dispersions with variable ranges of attractions.

Figure 4 shows the effect of the reduced critical temperature ($T_c^* = kT_c/\varepsilon$) as a function of the range of attraction (Γ) for six model potentials of colloids. Here the RG results for the square-well potential are from Lue and Prausnitz [74]. As introduced by Noro and Frenkel [43], the range of attraction for an arbitrary potential is defined as that for an effective square-well potential that yields the same reduced second virial coefficient at the same reduced temperature. For colloids with short-ranged attractions ($\Gamma < 0.4$), the simulation points remarkably fall into a straight line as proposed by Noro and Frenkel [43]:

$$T_c^* = 0.26 + 2.1\Gamma. \tag{24}$$

While for the Yukawa fluids the critical temperatures predicted by the RG theory (the solid line) agree well with that from Eq. (24), when the range of attraction is larger than 0.4, the critical temperatures of the square-well fluids calculated from the RG theory and from the Monte Carlo simulation clearly do not follow the simple linear relation. The deviation is most significant at large values of the range of attractions.

We found that the invariance of the reduced second virial coefficients ($B_2^* = B_2/B_2^{HS}$) at the critical point of fluid-fluid transition is not supported by the RG calculations at least for the Yukawa and the square-well fluids. Indeed, it has been shown before by Rosenbaum and co-workers that at the critical point of the metastable fluid-fluid equilibrium, the reduced osmotic second virial coefficients of protein solutions remain sensitive to the solution conditions [11]. Figure 5 plots B_2^* vs Γ, using results from RG calculations and from the Monte Carlo simulations. At small values of Γ where the

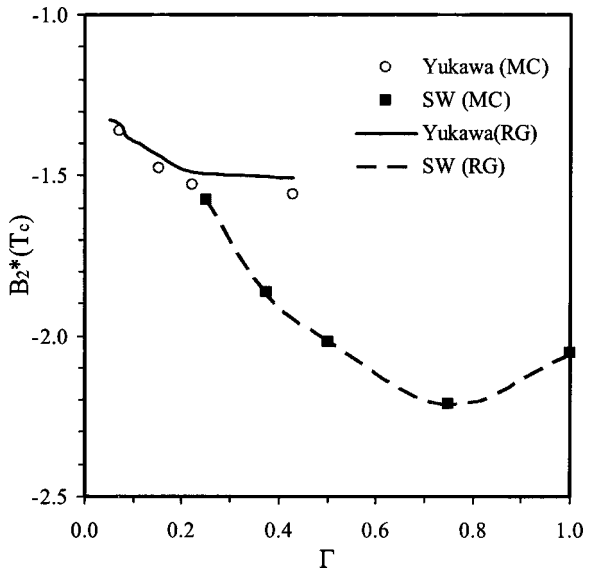

FIG. 5. The reduced second virial coefficient at the fluid-fluid critical point for the Yukawa potential and for the square-well potential. The points are simulation results from Vliegenthart and Lekkerkerker [44], and the solid lines are calculated, using the RG theory. The RG results for the square-well potential are from Lue and Prausnitz [74].

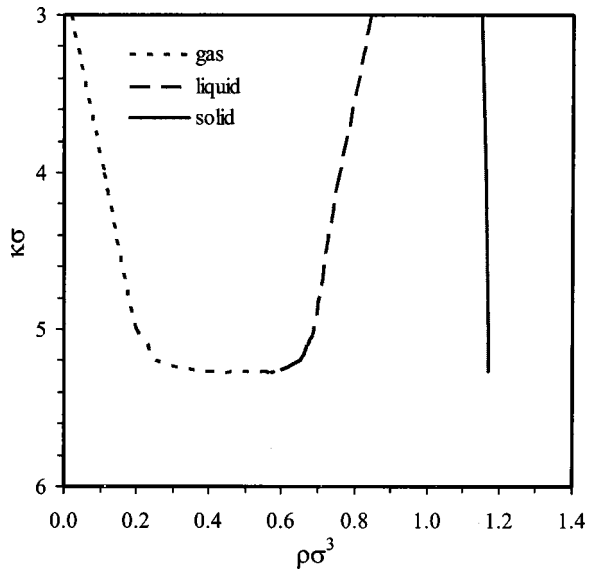

FIG. 6. The reduced densities of vapor, liquid, and solid phases at the triple points of the Yukawa model system at various ranges of attractions.

attractive potential is short ranged, the reduced second virial coefficient declines as Γ increases. Interestingly, B_2^* exhibits a minimum at an intermediate range of attractions for the square-well potential. There has been speculation that the low values of the reduced second virial coefficient at the critical point of protein solutions are associated with the strong anisotropic attractions between protein particles [8,78]. However, Fig. 5 implies that at certain conditions, an isotropic potential may also give a relative small value of B_2^*.

C. Threshold of the range of attraction for a stable fluid-fluid transition

It is now well known that the range of attraction between particles determines whether or not a colloidal system can exhibit a stable fluid-fluid transition. However, it remains difficult to quantitatively predict the range of attraction beyond which the fluid-fluid transition is thermodynamically stable. Recently, Noro and Frenkel observed that for $2n-n$ Lennard-Jones potential, α-Lennard-Jones potential, and attractive Yukawa potential, the boundary between stable and metastable fluid-fluid transition is located within a narrow range of Γ between 0.13 and 0.15 [43].

By using the RG theory and perturbation theories for fluid and solids, we calculated the triple points of the Yukawa and AO fluids at different ranges of attractions. The triple point disappears when the fluid-fluid transition becomes metastable in comparison to the fluid-solid equilibrium. Figure 6 shows the dependence of the triple point densities on the screening parameters of the attractive Yukawa potential. When the attraction is long ranged (small values of $\kappa\sigma$), the triple point resembles that for a simple fluid where the densities of vapor, liquid, and solid are easily distinguishable. The densities of ''vapor'' and ''liquid'' phases converges as the range of attraction decreases and when $\kappa\sigma > 5.3$, the triple point disappears, signaling a metastable fluid-fluid transition. This value of $\kappa\sigma$ corresponds to the range of attraction $\Gamma = 0.13$ at the critical point, in excellent agreement with the simulation result.

Figure 7 presents the triple points of the AO potential at different values of the polymer-particle size ratios. The crossover size ratio predicted by the RG theory ($\delta = 0.45$) is slightly larger than that obtained form direct simulations based on the AO potential ($\delta = 0.4$). This discrepancy is likely related to the inaccuracy of our theory for predicting the freezing line of the AO fluid with short-ranged attractions. Based on a model polymer-colloid system consisting

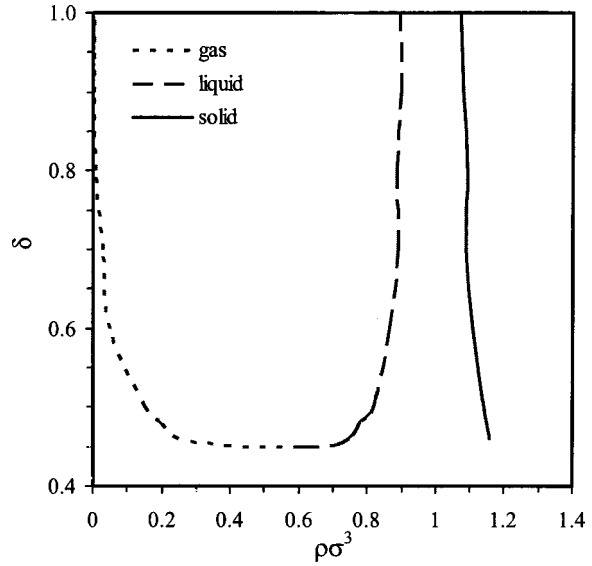

FIG. 7. The triple points for the Asakura-Oosawa system.

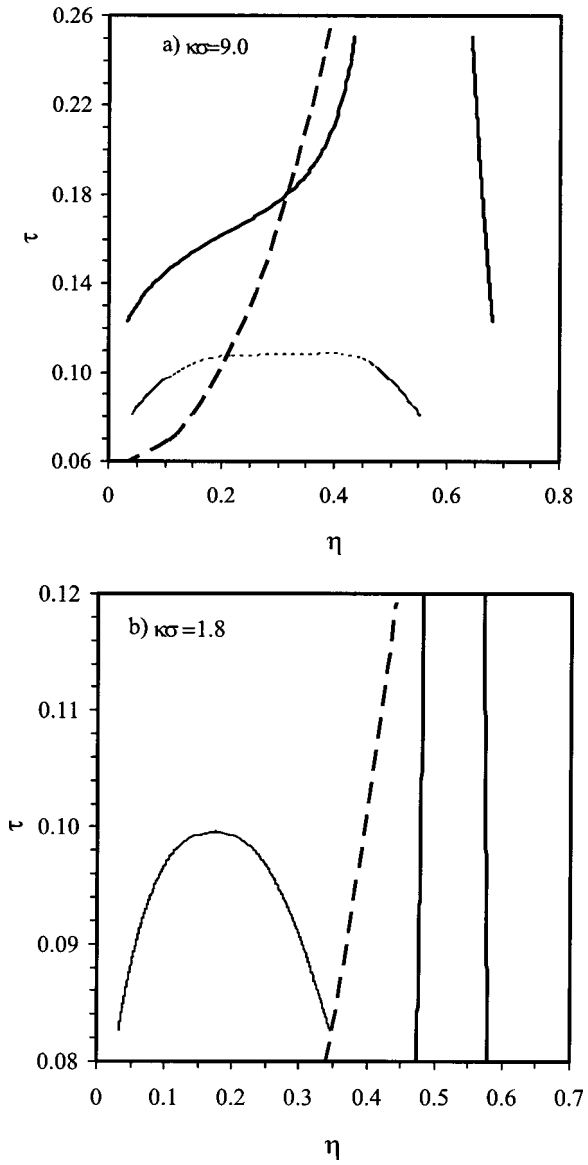

FIG. 8. (a) The fluid-fluid coexistence (thin broken line), the fluid-solid coexistence (solid line), as well as the percolation line (dashed line) for the Yukawa potential at $\kappa\sigma=9.0$. (b) Same as (a) but for $\kappa\sigma=1.8$. Here the fluid-fluid transition is thermodynamically stable and is labeled as the thin solid line.

of poly(methyl methacrylate) particle and polystyrene polymers, the experimental value for the crossover size ratio is about 0.24, significantly lower than the prediction of most current calculations. This disagreement between the theory and experiments warrants further investigations. Because it is not obvious on how to define the reduced temperature in terms of the AO potential, we did not compare the onset range of attraction with the empirical rule proposed by Noro and Frenkel [43].

D. Gelation

Figure 8 presents the phase diagrams of the Yukawa system at variable ranges of attractions. Also shown in this figure is the percolation line predicted using Eq. (20). Gelation is likely to occur underneath the percolation line. When the attraction is short-ranged, the percolation line crosses both the freezing line and the metastable fluid-fluid coexistence curve. Above the percolation line, crystallization and metastable fluid-fluid transition are expected to be observable. Conversably, below the percolation line, gelation may occur before crystallization or the metastable fluid-fluid separation. As the range of attraction increases, the percolation line shifts to the right-hand side of the phase diagram. As a result, gelation becomes less likely to interfere with the crystallization and the fluid-fluid transitions. Because colloidal particles are often larger than protein molecules and the attraction between colloidal particles is relatively shorter ranged in comparison to that between proteins, Fig. 8 explains in part why metastable fluid-fluid transition is often observed in aqueous protein solutions, but not in typical colloids. Similar equilibrium and nonequilibrium phase boundaries have been reported by Kulkarni and co-workers for square-well systems and for aqueous protein solutions [8].

For systems with long-ranged attractions, the fluid-fluid transition becomes thermodynamically stable and the gelation line shifts out of the fluid-fluid coexistence region [Fig. 8(b)]. As the range of attraction is further increased, we expect that the percolation line will move further toward the right-hand side of the melting line. In that event, both the fluid-fluid and fluid-solid transitions are free from the interference of the percolation. As a result, the fluid-fluid transition and freezing should be readily observable as in a simple fluid where the intermolecular attractions are long ranged. The interplay between the equilibrium phase behavior and gelation, as shown in Fig. 8, agrees at least qualitatively with that reported by Foffi and co-workers based on SCOZA for the fluid phases and MCT for gelation [17].

Similar phase behavior is observed using the AO potential (Fig. 9). Interestingly, we found that, as shown in Fig. 9(a), the percolation line may interfere only with the metastable fluid-fluid transition, but not with the freezing line for the AO system with short-ranged attractions. In comparison to that in the Yukawa system with also short-ranged attractions [Fig. 8(a)], it appears that crystallization in colloidal systems is sensitive to the specific forms of the attractive potential. Figure 9(b) shows that in the AO system, the percolation line may impede the fluid-fluid equilibrium, freezing as well as melting transitions.

IV. CONCLUSIONS

Over the last decade there have been extensive investigations on the relation between the osmotic second virial coefficient and the phase behavior of colloids, solubility and crystallization of proteins in aqueous solutions in particular. We have shown that at the critical point of the fluid-fluid transition, the osmotic second virial coefficient varies with the range of attractions, in contrast to the common belief that it remains practically constant. However, given an accurate pair potential of mean force between colloidal particles, statistical-mechanical theories in complement with the RG correction may provide reliable equilibrium phase diagrams

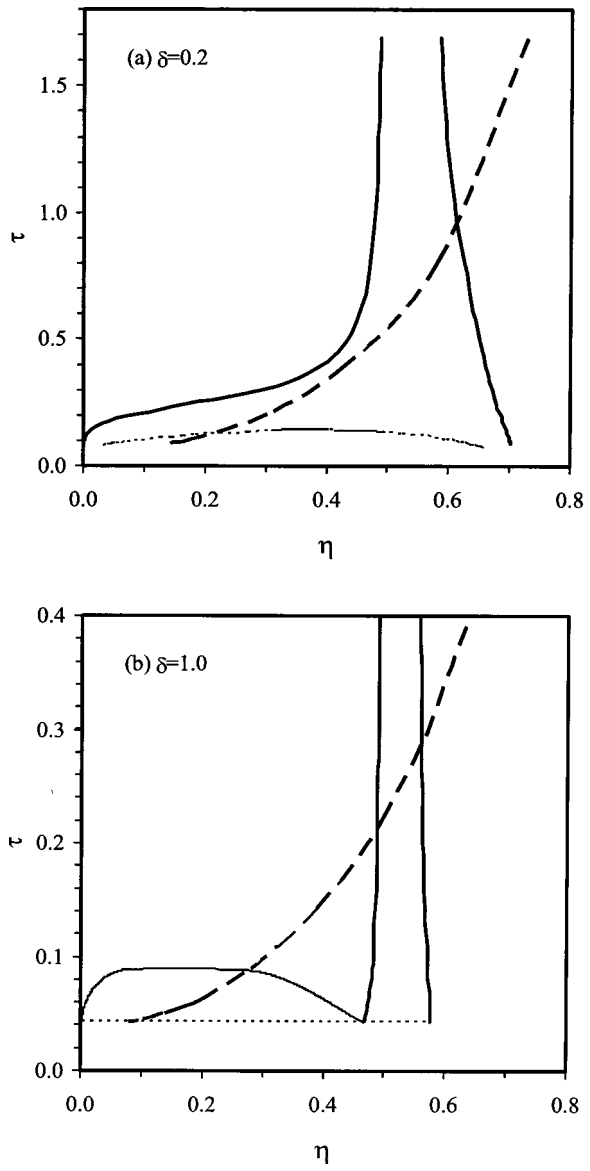

FIG. 9. Same as Fig. 8 but for the Asakura-Oosawa potential. (a) $\delta=0.2$ and (b) $\delta=1.0$.

of colloids (with the premise that the potential of mean force is pairwise additive).

For colloids with short-ranged attractions, the critical temperature of the fluid-fluid transition appears well correlated with the range of attractions, essentially independent of the details of the potential profiles. Such correlation will be useful for the estimation of the critical temperature of colloidal dispersions once the potential profile or the osmotic second virial coefficient is already known. Since the latter can be conveniently measured using conventional light scattering or chromatography methods [79], a correlation on the critical temperature and the range of attraction may find applications in the identification of favorable solutions conditions leading toward protein crystallization. As observed by Noro and Frenkel [43], the range of attraction may also provide a convenient parameter to justify whether or not the fluid-fluid transition is thermodynamically stable.

By comparing the relative positions of the phase coexistence curves and the percolation lines in the same phase diagram, we conclude that gelation is most likely to occur for systems with short-ranged attractions. The interaction between gelation and the equilibrium phase transitions depend not only on the range of attractions but also on the details of the potential profiles. Because percolation is a necessary but not sufficient condition leading to gelation or glass transitions, further investigations are required to understand the interplay among equilibrium and nonequilibrium phase transitions, glass transitions in particular.

ACKNOWLEDGMENTS

D. Fu and Y. Li gratefully acknowledge the financial support from the Fundamental Research Fund of Tsinghua University, Beijing (Grant No. JZ2002003). J. Wu is grateful for the support from the University of California Directed Research and Development Program.

APPENDIX A

The following definitions are used to calculate the Helmholtz energy of Yukawa fluids according to the modified MSA. The parameters θ_0 and Φ_0 in Eq. (2) are given by

$$\theta_0=\frac{\Theta(\lambda)}{\lambda^2(1-\eta)^2}, \tag{A1}$$

$$\Phi_0=\frac{e^{-\lambda}\Theta(\lambda)+S(\lambda)}{\lambda^3(1-\eta)^2}, \tag{A2}$$

and the single-variable function $F(x)$ is

$$F(x)=-\frac{1}{4}\ln(1-2x)-2\ln(1-x)-\frac{3}{2}x-\frac{1}{1-x}+1, \tag{A3}$$

where $\lambda=\kappa\sigma$ and

$$\Theta(\lambda)=12\eta[(1+\eta/2)\lambda+1+2\eta], \tag{A4}$$

$$S(\lambda)=(1-\eta)^2\lambda^3+6\eta(1-\eta)\lambda^2+18\eta^2\lambda-12\eta(1+2\eta), \tag{A5}$$

$$x=\frac{6\eta(1+\lambda\phi)}{\Phi_0^2\lambda^2}\frac{\varepsilon}{kT}, \tag{A6}$$

$$y=\frac{6\eta\phi}{\Phi_0^2\lambda}\frac{\varepsilon}{kT}, \tag{A7}$$

$$\phi=\frac{\lambda^2(1-\eta)^2(1-e^{-\lambda})-12\eta(1-\eta)[1-\lambda/2-(1+\lambda/2)e^{-\lambda}]}{e^{-\lambda}\Theta(\lambda)+S(\lambda)}. \tag{A8}$$

APPENDIX B

The RG calculations in this work follow the recursion relations reported by Jiang and Prausnitz [80]. The differential Helmholtz energy density is given by

$$\delta f_n(\rho)=\begin{cases} K_n \ln\dfrac{\Omega_i^n}{\Omega_s^n}, & 0\leqslant\rho<\rho_{\max}/2 \\ 0, & \rho_{\max}/2\leqslant\rho<\rho_{\max}, \end{cases} \tag{B1}$$

where $\rho_{\max}$ is the maximum possible particle number density and

$$K_n=\frac{kT}{2^{3n}L^3}, \tag{B2}$$

$$\Omega_i^n(\rho)=\int_0^\infty \exp[-G_i^n(\rho,x)/K_n]dx, \quad i=s,\ l, \tag{B3}$$

$$G_i^n(\rho,x)=\frac{\overline{f_i^n}(\rho+x)+\overline{f_i^n}(\rho-x)-2\overline{f_i^n}(\rho)}{2}, \quad i=s,\ l, \tag{B4}$$

$$\overline{f_i^n}(\rho)\approx f_{n-1}(\rho)+a\rho^2, \tag{B5}$$

$$\overline{f_s^n}(\rho)=f_{n-1}(\rho)+a\rho^2\frac{\psi\overline{\omega}^2}{2^{2n+1}\overline{L}^2}, \tag{B6}$$

$$a=\frac{1}{2}\int u_A(|\mathbf{r}-\mathbf{r}'|)d\mathbf{r}, \tag{B7}$$

$$\overline{L}=L/\sigma, \tag{B8}$$

$$\overline{\omega}^2=\frac{1}{3!a\sigma^2}\int r^2 u_A(|\mathbf{r}-\mathbf{r}'|)d\mathbf{r}. \tag{B9}$$

For the model potentials considered in this work, we find that the parameter $\overline{\omega}^2$ is

$$\overline{\omega}^2_{yuk}=\frac{1}{3}\left(\frac{6+6\lambda+3\lambda^2+\lambda^3}{\lambda^2(1+\lambda)}\right). \tag{B10}$$

for Yukawa fluids and

$$\overline{\omega}^2_{AO}=\frac{1}{3}\left(\frac{-1/5+a_1/6-a_2/8+(1+\delta)^5/5-a_1(1+\delta)^6/6+a_2(1+\delta)^8/8}{-1/3+a_1/4-a_2/6+(1+\delta)^3/3-a_1(1+\delta)^4/4+a_2(1+\delta)^6/6}\right). \tag{B11}$$

for AO fluids.

[1] A. P. Gast and W. B. Russel, Phys. Today **51**(12), 24 (1998).
[2] W. Poon, P. Pusey, and H. Lekkerkerker, Phys. World **9**(4), 27 (1996).
[3] K. M. Kulinowski *et al.*, Adv. Mater. (Weinheim, Ger.) **12**, 833 (2000).
[4] V. J. Anderson and H. N. W. Lekkerkerker, Nature (London) **416**, 811 (2002).
[5] Y. N. Xia *et al.*, Adv. Mater. (Weinheim, Ger.) **12**, 693 (2000).
[6] S. T. Yau *et al.*, J. Mol. Biol. **303**, 667 (2000).
[7] H. W. Blanch *et al.*, Fluid Phase Equilib. **194**, 31 (2002).
[8] A. M. Kulkarni, N. M. Dixit, and C. F. Zukoski, Faraday Discuss. **123**, 37 (2003).
[9] P. M. Tessier *et al.*, Proteins: Struct., Funct., Genet. **50**, 303 (2003).
[10] R. Piazza and M. Pierno, J. Phys.: Condens. Matter **12**, A443 (2000).
[11] D. F. Rosenbaum *et al.*, J. Chem. Phys. **111**, 9882 (1999).
[12] S. Ramakrishnan and C. F. Zukoski, J. Chem. Phys. **113**, 1237 (2000).
[13] D. C. Prieve, Adv. Colloid Interface Sci. **82**, 93 (1999).
[14] J. L. Anderson, D. Velegol, and S. Garoff, Langmuir **16**, 3372 (2000).
[15] J. Y. Walz, Adv. Colloid Interface Sci. **74**, 119 (1998).
[16] M. G. Noro, N. Kern, and D. Frenkel, Europhys. Lett. **48**, 332 (1999).
[17] G. Foffi *et al.*, Phys. Rev. E **65**, 031407 (2002).
[18] V. J. Anderson, E. H. A. de Hoog, and H. N. W. Lekkerkerker, Phys. Rev. E **65**, 011403 (2002).
[19] A. P. Gast, C. K. Hall, and W. B. Russel, J. Colloid Interface Sci. **96**, 251 (1983).
[20] M. Baus and R. Achrayah, J. Phys.: Condens. Matter **8**, 9633 (1996).
[21] F. Fornasiero, J. Ulrich, and J. M. Prausnitz, Chem. Eng. Process. **38**, 463 (1999).
[22] L. Mederos, J. Mol. Liq. **76**, 139 (1998).
[23] H. Mahadevan and C. K. Hall, AIChE J. **36**, 1517 (1990).
[24] M. H. J. Hagen *et al.*, Nature (London) **365**, 425 (1993).
[25] M. H. J. Hagen and D. Frenkel, J. Chem. Phys. **101**, 4093 (1994).

[26] M. Dijkstra, J. M. Brader, and R. Evans, J. Phys.: Condens. Matter **11**, 10079 (1999).
[27] L. Mederos and G. Navascues, J. Chem. Phys. **101**, 9841 (1994).
[28] A. Vrij *et al.*, Faraday Discuss. **90**, 31 (1990).
[29] H. Mahadevan and C. K. Hall, Fluid Phase Equilib. **78**, 297 (1992).
[30] N. Asherie, A. Lomakin, and G. B. Benedek, Phys. Rev. Lett. **77**, 4832 (1996).
[31] M. Dijkstra, Phys. Rev. E **66**, 021402 (2002).
[32] K. A. Dawson, Curr. Opin. Colloid Interface Sci. **7**, 218 (2002).
[33] W. B. Russel, D. A. Saville, and W. R. Schowalter, *Colloidal Dispersions* (Cambridge University Press, Cambridge, 1989).
[34] V. Trappe *et al.*, Nature (London) **411**, 772 (2001).
[35] W. Hartl, Curr. Opin. Colloid Interface Sci. **6**, 479 (2001).
[36] U. Bengtzelius, W. Gotze, and A. Sjolander, J. Phys. C **17**, 5915 (1984).
[37] W. Vanmegen and S. M. Underwood, Phys. Rev. Lett. **70**, 2766 (1993).
[38] K. N. Pham *et al.*, Science **296**, 104 (2002).
[39] G. F. Wang and S. K. Lai, Phys. Rev. Lett. **82**, 3645 (1999).
[40] K. A. Dawson *et al.*, J. Phys.: Condens. Matter **13**, 9113 (2001).
[41] A. M. Puertas, M. Fuchs, and M. E. Cates, Phys. Rev. Lett. **88**, 098301 (2002).
[42] D. Rosenbaum, P. C. Zamora, and C. F. Zukoski, Phys. Rev. Lett. **76**, 150 (1996).
[43] M. G. Noro and D. Frenkel, J. Chem. Phys. **113**, 2941 (2000).
[44] G. A. Vliegenthart and H. N. W. Lekkerkerker, J. Chem. Phys. **112**, 5364 (2000).
[45] B. Guo *et al.*, J. Cryst. Growth **196**, 424 (1999).
[46] J. A. White and S. Zhang, J. Chem. Phys. **103**, 1922 (1995).
[47] J. A. White and S. Zhang, J. Chem. Phys. **99**, 2012 (1993).
[48] Y. C. Chiew and E. D. Glandt, J. Phys. A **22**, 3969 (1989).
[49] J. P. Hansen and I. R. McDonald, *Theory of Simple Liquids* (Academic, London, 1990).
[50] L. Blum and J. S. Hoye, J. Stat. Phys. **19**, 317 (1978).
[51] E. Lomba and N. G. Almarza, J. Chem. Phys. **100**, 8367 (1994).
[52] D. Henderson, L. Blum, and J. P. Noworyta, J. Chem. Phys. **102**, 4973 (1995).
[53] D. Henderson, L. Mier-Y-Teran, and L. Blum, Fluid Phase Equilib. **130**, 65 (1997).
[54] D. M. Duh and L. Mier-Y-Teran, Mol. Phys. **90**, 373 (1997).
[55] N. F. Carnahan and K. E. Starling, J. Chem. Phys. **51**, 635 (1969).
[56] Z. P. Liu, Y. G. Li, and K. Y. Chan, Ind. Eng. Chem. Res. **40**, 973 (2001).
[57] Y. Z. Lin, Y. G. Li, and J. F. Lu, J. Colloid Interface Sci. **239**, 58 (2001).
[58] W. C. K. Poon, J. Phys.: Condens. Matter **14**, R859 (2002).
[59] S. Asakura and F. Oosawa, J. Chem. Phys. **22**, 1255 (1954).
[60] R. Dickman, P. Attard, and V. Simonian, J. Chem. Phys. **107**, 205 (1997).
[61] J. Chang and S. I. Sandler, Mol. Phys. **81**, 735 (1994).
[62] L. Verlet and J. J. Weis, Phys. Rev. A **5**, 939 (1972).
[63] F. W. Tavares and S. I. Sandler, AIChE J. **43**, 218 (1997).
[64] J. Z. Wu, G. Huang, and Z. B. Hu, Macromolecules **36**, 440 (2003).
[65] J. Z. Wu and J. Prausnitz, Fluid Phase Equilib. **194**, 689 (2002).
[66] J. E. Lennard-Jones and A. F. Devonshire, Proc. R. Soc. London, Ser. A **163**, 53 (1937).
[67] C. Rascon, L. Mederos, and G. Navascues, Phys. Rev. E **54**, 1261 (1996).
[68] E. Velasco, L. Mederos, and G. Navascues, Langmuir **14**, 5652 (1998).
[69] J. D. Hirschfelder, C. F. Curtis, and R. B. Bird, *Molecular Theory of Gases and Liquids* (Wiley, New York, 1964).
[70] J. V. Sengers, *Equations of State for Fluids and Fluid Mixtures*, International Union of Pure and Applied Chemistry. Commission on Thermodynamics (Elsevier, Amsterdam, 2000).
[71] M. Muschol and F. Rosenberger, J. Chem. Phys. **107**, 1953 (1997).
[72] N. Asherie, A. Lomakin, and G. B. Benedek, Biophys. J. **82**, 317a (2002).
[73] P. R. tenWolde and D. Frenkel, Science **277**, 1975 (1997).
[74] L. Lue and J. M. Prausnitz, J. Chem. Phys. **108**, 5529 (1998).
[75] Y. P. Tang, J. Chem. Phys. **109**, 5935 (1998).
[76] J. W. Jiang and J. M. Prausnitz, AIChE J. **46**, 2525 (2000).
[77] J. W. Jiang and J. M. Prausnitz, Fluid Phase Equilib. **169**, 127 (2000).
[78] R. P. Sear, Phys. Rev. E **61**, 651 (2000).
[79] P. M. Tessier, A. M. Lenhoff, and S. I. Sandler, Biophys. J. **82**, 1620 (2002).
[80] J. W. Jiang and J. M. Prausnitz, J. Chem. Phys. **111**, 5964 (1999).
[81] K. P. Shukla, J. Chem. Phys. **112**, 10358 (2000).